

Electron-beam accelerator for pumping of a Xe₂ lamp

B.M. KOVALCHUK, A.V. KHARLOV, S.N. VOLKOV, A.A. ZHERLITSYN, V.B. ZORIN,
G.V. SMORUDOV, AND V.N. KISELEV

Institute of High-Current Electronics, Siberian Division of Russian Academy of Sciences, Tomsk, Russia

(RECEIVED 11 July 2011; ACCEPTED 7 October 2011)

Abstract

A high-current electron-beam accelerator for pumping of a Xe₂ lamp was developed. It is intended for injection of an electron beam into cylindrical gas cavity (diameter of 400 mm, length of 1600 mm, and the absolute pressure up to 3 bars). Two electron diodes in parallel are used in the accelerator. Each diode is connected to a linear transformer driver with vacuum insulation of a secondary turn. The next parameters of the accelerator have been obtained: diode voltage — 550–600 kV, diode current — 276–230 kA, current rise time — 160 ns, maximum power of the electron beam — 130 GW, pulse width on half maximum — 160 ns, electron beam energy at power level not less than half of maximum value — 20 kJ. The total energy of electrons, which pass through a 40 μm Ti foil into the Xe cell, is 8–9 kJ in the 150–160 ns pulse (full width at half maximum) mean specific power of energy input into gas cavity is about 330 kW/cm³. Design of the accelerator and test results are presented and discussed in this paper.

Keywords: Electron beam; Laser; Linear transformer

INTRODUCTION

High-current, large-area electron beams are used to energize large gas lasers for inertial fusion research and other applications. The electron beam is usually generated from an explosive emission cold cathode and extracted into a lasing gas through a thin metallic foil. Detailed investigation of several types of passive and active cathodes (metal ceramic, velvet, carbon fiber, multicapillary and multislotted cathodes, and active ferroelectric and hollow anodes plasma sources) was reported by Krasik *et al.* (2009). The cathodes are typically driven by pulsed power generators of 500–700 kV voltage and of hundreds of kiloamperes, with pulse duration up to 1 μs. Maximizing the electron-beam energy deposited into the gas (assuming that it is below saturation level) is required to maximize the pump efficiency, as well as minimizing the electron-beam energy deposited in foils, and anode ribs to ensure the survivability of the foils and to minimize the heat dissipation requirements. Two powerful KrF lasers, Electra and Nike were developed for inertial fusion energy research at the United States Naval Research Laboratory. Electra is a high average power laser, which employs two counter-propagating electron beams for pumping of a laser cell, each beam of a 500 KeV, 100 kA, 150 ns, and area

30 × 100 cm² at repetition rate of 5 Hz (Sethian *et al.*, 2000; Myers *et al.*, 2004). The Nike laser amplifier produces opposing 750 kV, 500 kA, 240 ns, 60 × 200 cm² electron beams (Sethian *et al.*, 1997; Karasik *et al.*, 2010). In both these installations (Electra and Nike), each electron beam is produced by its own Marx generator and pulse forming line system.

Linear transformer driver (LTD) technology is actively developed since 1997 at the Institute of High Current Electronics in Tomsk, Russia (Kim *et al.*, 1999; Baskrikov *et al.*, 2003; Kovalchuk *et al.*, 2009a). The LTD driver is an induction generator similar to the linear induction accelerator (LIA), the inductive voltage adder (IVA), and the linear pulsed transformer (LPT). Excellent review on induction generators is given by Smith (2004). All induction generators are based on Faraday's law, which states that the time-varying magnetic flux $B(t)$ penetrating a loop generates at the ends of this loop a voltage difference $U(t)$ equal to $U(t) = SdB/dt$ where S is the cross-section of the loop. In an induction generator, normally the loop is realized as a pillbox-shaped toroid, which is usually called "induction cavity." This toroid has a continuous azimuthal gap, and the voltage $U(t)$ appears across this gap. Historically, the first devices utilizing Faraday's law were called "transformers," all induction generators can also be considered as transformers. LIA, IVA, and LPT can be formed by one or a series of identical induction cavities. In LIA, a central

Address correspondence and reprint requests to: A.V. Kharlov, 2/3 Akademicheskoy Ave., 634055, Tomsk, Russia. E-mail: akharlov@lef.hcei.tsc.ru

bore is threaded by a beam of propagating particles, which gets accelerated as they drift through each of the cavity gaps. IVA is also formed by a series of identical induction cavities, but unlike in LIA, its bore is threaded by a center conductor that together with the cylindrical surface of the bore forms an output line that connects to the load.

Similar to IVA and LPT, the LTD driver consists of several induction cavities called “LTD stages” plus the center electrode threading through the axis of the cavities. The main difference from LIA, IVA, and LPT induction cavities is that the LTD stage encloses the primary capacitive energy storage. Simplified schematics of the LTD assembly are presented in Figure 1. One can see in Figure 1 that capacitors (C), switches (S), and ferromagnetic cores (F) are directly incorporated into the LTD stages to generate a fast output voltage pulse, which is added along a vacuum coaxial line. So, the LTD technique allows one to eliminate intermediate pulse forming elements and could be quite competitive with other types of generators on the same output voltage. Another advantage is that body of the LTD cavity keeps ground potential during the shot and it allows assembling them in series or in parallel depending on load requirements. Pulse length and current amplitude of a LTD assembly are defined mainly by parameters of one stage, and output voltage is directly proportional to the number of stages.

Recent development of high voltage low inductance capacitors and low inductance switches enabled to achieve about 100 ns rise time of the LTD output pulse (Kim *et al.*, 2009). High-current accelerator, based on linear transformer driver technology, for pumping of the 200-L excimer laser was developed at the Institute of High Current Electronics, providing electron energy of 550 keV, a diode current of 320 kA, and an e-beam current of 250 kA (Kovalchuk *et al.*, 2003). The present paper describes a new electron accelerator, driven by two generators, each of them consisting of 12 LTD stages. Implementation of new technology enabled us to increase rate of the diode power rise from 0.5 GW/ns in (Kovalchuk *et al.*, 2003) to 1 GW/ns in the described generator at almost the same level of the output power. This accelerator is intended for pumping of the Xe₂ lamp for hybrid femtosecond XeF (C-A) laser system.

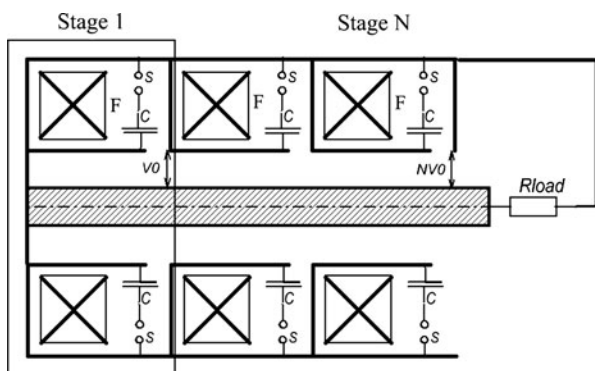


Fig. 1. Principal schematics of the LTD assembly.

A photochemically driven XeF(C-A) gain medium is now considered as an alternative to existing solid state active media for femtosecond pulse amplifiers (Tcheremiskine *et al.*, 2002; Zvorykin *et al.*, 2008).

DESIGN OF THE ACCELERATOR

Block scheme of the generator is given in Figure 2. At command from a control computer capacitor blocks of 12 stages of two linear transformers are charged from a high voltage (HV) power supply up to 90–100 kV. The same power supply charges a capacitor block of the triggering generator. Capacitors of the Marx generator are charged up to 20 kV from a thyatron generator. A delay block forms signal for triggering of a premagnetization generator. At about 100 μs after triggering (at maximum of the premagnetization current) signal from the delay block triggers the thyatron generator, which in turn triggers the Marx generator. Voltage from the Marx generator output is delivered for triggering of the capacitor block switch of the triggering generator. Voltage from the triggering generator output fires switches of the capacitor blocks of the linear transformer stages. Voltage from the linear transformer outputs is delivered to the cathodes of a vacuum diode, placed on both sides of a gas cavity. Electrons beams, generated in two diodes, are injected into the gas volume through Ti foil, fixed on the anode ribs, and pump a working gas.

Assembling drawing of the electron accelerator is given in Figure 3. Two HV pulse generators, made on scheme of a linear transformer with vacuum electric insulation of a secondary turn, are used to drive the electron diode. Each generator consists of 12 LTD stages, with 8 capacitor GA35426 (100 kV, 40 nF) in each stage. HV pulse generators are placed on both sides of the vacuum chamber (4), where the vacuum electron diode and pumped gas volume are installed. Transformer stages are connected in series and hermetically sealed in between through the acryl insulators (3). Central conductor (6), placed inside the stages, serves as part of a secondary turn for all 12 LTD stages. One end of this conductor is connected with the cathode of

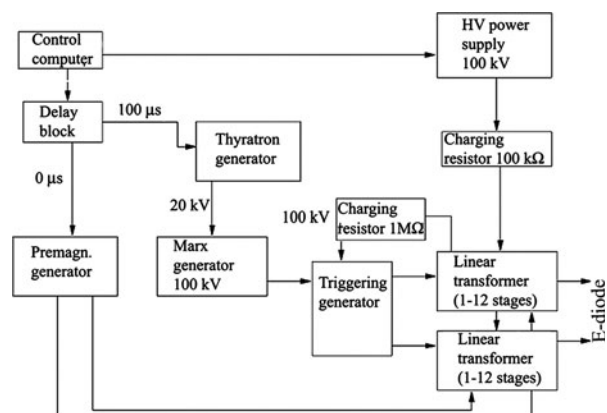


Fig. 2. Block scheme of the installation.

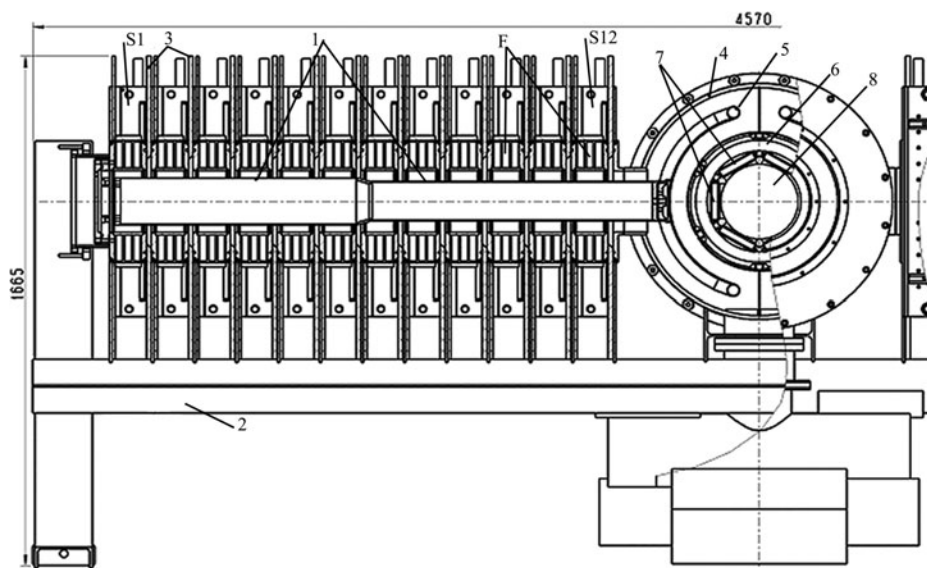


Fig. 3. Assembling drawing of the accelerator: (1) central conductor, (2) basement, S1-S12 — 12 LTD stages, F = ferromagnetic cores, (3) acrylic insulators, (4) body of the vacuum chamber, (5) cathode, (6) Xe volume, (7) CaF_2 windows of a laser cell, (8) laser cell.

the electron diode, the other one is fixed on a flange of the first stage of the linear transformer. Central conductor (6) is made as cylinder with variable diameter of 160/140 mm. In Figure 3, there are 12 LTD stages—primary turns (S1-S12). These primary turns are air insulated (electrically). Secondary turn is formed in Figure 3 by central conductor (6), electron diode and inner conductor of the stages housing. High voltage is localized here in vacuum coaxial, and vacuum insulation of a secondary turn directly means that electric field strength on the central conductor (6) is below vacuum breakdown level and magnetic insulation is not necessary. Synchronization and triggering systems provide synchronous firing of all 24 LTD stages of the accelerator.

DESIGN OF THE TRANSFORMER STAGE

Capacitor block is a main structural element of the transformer stage. Design of the capacitor block is given in Figure 4. It incorporates two capacitors GA 35426 (40 nF, 100 kV) and multichannel multigap gas switch. Body (1) of the block is founded from epoxy compound. A cavity for a switch placement (Fig. 4c) is formed in the block body during casting. Capacitors (2) are sealed within epoxy in the block body permanently. Epoxy sealing enhances external electric insulation of the capacitors and provides possibility of operation at 100 kV charging voltage in atmospheric air. Inner capacitors terminals are connected with the switch HV electrode 4. A multichannel gas switch was developed for use in the capacitor block. It is plane geometry switch with seven gaps in one channel and six channels in parallel. The switch (Fig. 4b) is assembled on the epoxy slab 3. The switch contains 36 ball electrodes (ball bearings steel, 22.3 mm in diameter). Voltage divider 9, assembled from film resistors on 68 M Ω , provides voltage distribution

between rows of electrodes. Triggering pulse is supplied to the second row of ball electrodes through capacitive coupling between the triggering cable 7 and ball electrodes. At arrival of a triggering pulse with polarity, opposite to the main pulse, homogeneous voltage distribution is distorted and gaps break down sequentially. Detailed description of the capacitor block and its tests are given in (Zherlitsyn *et al.* 2009; Kovalchuk *et al.* 2009b).

Module of the transformer stage is assembled from two capacitor blocks, connected in parallel. Blocks are placed on basement from a steel profile (position 5, Fig. 5) and fixed by plate (4) through (3) polyamide bolts (6). Charging voltage is supplied to the top block in the module through the transition insulator. Transition insulator is also installed between blocks for transferring of charging voltage to the other block.

Three-dimensional view of the *transformer stage* is given in Figure 5. The stage consists of two modules (M1 and M2), connected in parallel on a primary turn of the linear transformer, and inductor (F). The modules are placed on a mounting plate (1) symmetrically relatively to the plate center and fixed to the plate from low voltage side. High voltage terminals of the capacitor blocks are connected with combined current frame (3) through spring contacts. Acrylic insulator sheet (2) is placed between modules and mounting plate. It is important in this design that each module of the whole LTD assembly can be taken out separately in need of repair. Stage overall dimensions are 750 × 1510 × 132 mm².

Inductor of the transformer stage (F) is installed outside of outer conductor of a vacuum coaxial line. The inductor consists of three cores, assembled in polyethylene body. Each core is wound up by 18 mm strip from transformer steel ET 3425 (saturation field $B_s = 1.9$ T, reset or residual field $B_r = 1.4$ T, electrical resistivity 0.5×10^6 Ωm) with insulation by 10 μm Mylar tape between turns. Length of the

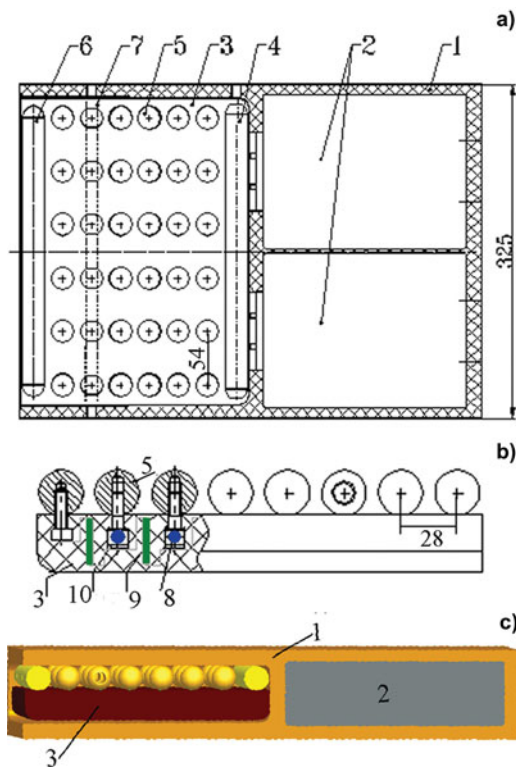


Fig. 4. (Color online) (a) Cross-section drawing of the capacitor block, (b) electrodes system assembly, (c) three-dimensional model cut view. Here shown: 1 = epoxy body, 2 = capacitors GA 35426, 3 = switch plate, 4 = HV electrode, 5 = ball switch electrodes, 6 = low voltage electrode, 7 = triggering cable, 8 = conductive cord, 9 = divider resistors, 10 = special screws for the balls mounting.

inductor middle core line is about 1 m; cross-section area of steel in the inductor three cores is about 40 cm², saturation value of a voltage-time product for the inductor about 13 mVs. Premagnetization is required because following

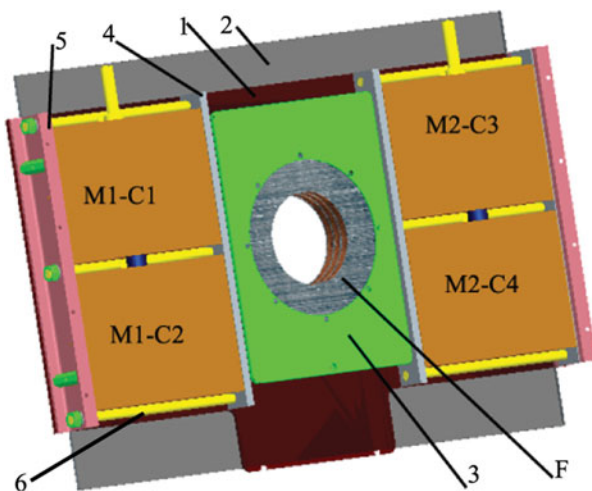


Fig. 5. (Color online) Three-dimensional view of a transformer stage: M1 and M2 = modules of the stage, C1-C4 = capacitor blocks of the modules, F = inductor, 1 = mounting plate, 2 = acryl insulator, 3 = central combined current frame, 4 = module fixing plate, 5 = module basement, 6 = caprolon rods.

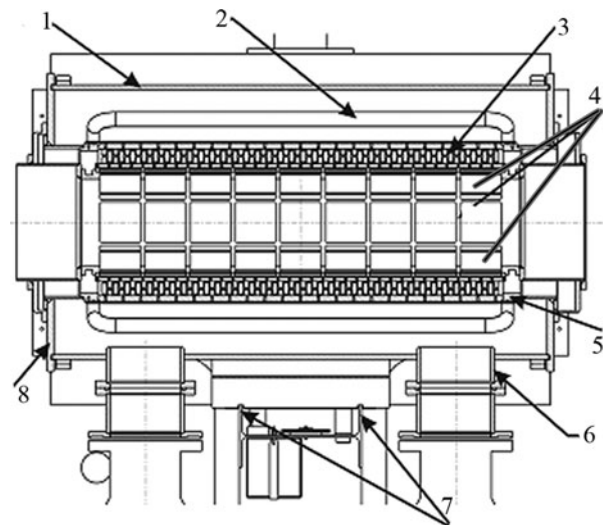


Fig. 6. Anode-cathode block: (1) vacuum chamber, (2) cathode, (3) Hibachi structure, (4) 9 sets of the CaF₂ windows along the laser cell, (5) anode, (6) vacuum pump, (7) horizontal alignment rails, (8) side flange.

main voltage pulse the ferromagnetic cores of stages have magnetic flux equal to $+Br$. The core must be reset to $-Br$ before the next pulse; otherwise, the stage will be short-circuited soon after the voltage is applied. Reverse biasing of the core is accomplished with a premagnetization circuit. The premagnetization circuit must have the following characteristics: (1) the circuit can generate an inverse voltage-time product greater than $(Bs + Br)S$ where S is cross-section of the inductor. (2) It can supply a unidirectional reverse current through the core axis of magnitude $Is > \pi d \times Hs$ where d is outer diameter of the inductor and Hs is magnetizing force of the core material.

Time-dependent response of ferromagnetic materials is considered in detail in book (Humphries, 1986).

DIODE DESIGN

Assembling drawing of the anode-cathode block is shown in Figure 6. Drawing of the vacuum chamber is given in Figure 7. The vacuum chamber is made as cylindrical vessel with inner diameter of 740 mm and length of 1440 mm. Two vertical stiffening plates, welded to the chamber wall at the top and bottom, hold the anode block. These plates also work as return current bus of the diode. Diameter of side flanges is 780 mm. System of the electron beam output from the diode into a gas cavity consists of a cylindrical framework (diameter of 440 mm, length 1400 mm, welded from stainless steel) with six windows 1210×160 mm² and six replaceable frames with Ti foil. The replaceable frame is made as perforated plate (stainless steel, $1210 \times 230 \times 3$ mm³), bent as a cylindrical surface with radius of 228 mm, and covered by the 40 μ m Ti foil. Working area of the frame (1145×160 mm²) is made as set of slots with width of 13 mm and step of 18 mm (usually it is

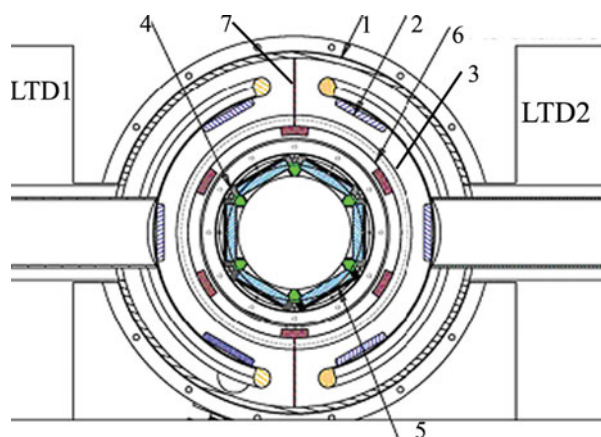


Fig. 7. (Color online) (1) Vacuum chamber, (2) cathodes, (3) anode, (4) 113 cm long hexahedral laser cell laser cell, (5) six rows of CaF_2 windows, (6) Xe chamber, (7) return current plate.

called as “hibachi” structure). The slots with length of 30 and 65 mm are cross-placed. Such structure provides high geometric transparency about 80% (very high value indeed) and high mechanical strength of the frame. Tests of the system were done at static pressure of 3 bars (absolute).

The hibachi must be as transparent as possible to the electron beam in order to maximize the electron deposition into the gas. It must also be able to withstand the static gas pressure and the cyclic hydrodynamic shocks induced as the electron beam deposits its energy into the gas. The foil must have a low enough area density to allow the electron beam to pass through efficiently. The foil itself must be damage resistant to electrons, X-rays, and ultraviolet light. Two common materials that meet these constraints are titanium and stainless steel.

The cathode structure is shown in Figure 8. The cathode holder of each diode is made as cylindrical panel from



Fig. 8. (Color online) Cathode structure: (1) safety frame, (2) cylindrical panel, (3) dielectric emitting surfaces.

stainless steel with a curvature radius of 284 mm. Edges of the cathode panel are enclosed in a rectangular protecting frame with dimensions $620 \times 1200 \text{ mm}^2$. There are three rectangular emitting surfaces on the cathode, flocked by dielectric with height of about 1–2 mm. The area of each emitting surface is $100 \times 1180 \text{ mm}^2$. Optimal value of the vacuum diode gap (distance between the cathode active surface and anode) is about 50–55 mm. The vacuum diode forms six 100 cm long \times 12 cm wide e-beams that are injected through a $40 \mu\text{m}$ Ti foil into the Xe converter. The 8 cm distance between Ti foil and CaF_2 windows was chosen to assure that the electrons will be stopped in the gas cavity at the xenon operating pressure of 3 bars.

EXPERIMENTAL RESULTS

Diagnostics

Active voltage dividers were used for the voltage measurement on the primary turn of each stage. Diode voltage is calculated taking into account inductances between each of the stages and the diode. The load and inductor currents were measured by inductive probes, installed in the last stage on both sides of the generator. Probe signals were acquired by Tektronix TDS 3054 digital oscilloscope (500 MHz, 4 channels, 5 Gs/s on each channel). Diode power, diode energy, diode impedance, dissipated energy in the inductor cores have been calculated from the measured signals. Set of calorimeters was used for estimation of the total beam energy and for control of the electron beam uniformity.

The local energy deposition rate in the gas can be determined by adding the contributions that appear as radiation and as heat, with the latter component manifested as a pressure rise. In a constant volume region, this pressure rise ΔP is related to the energy deposited as heat as $E_{\text{gas}} = \Delta P \times V_{\text{cell}} / (\gamma - 1)$ where γ is the ratio of the specific heat at constant pressure to that at constant volume and V_{cell} is the volume of the gas cell. The pressure rise in each experiment was measured using a 6MDX-3B transducer (it is vacuum tube with a moving electrode, where output current depends on displacement of the electrode and respectively on the pressure applied). According to the data presented in Eckstrom *et al.* (1988), ideal fluorescence efficiency of the e-beam pumped xenon is equal to 43%. In our geometry, VUV coupling efficiency, which is the product of CaF_2 windows transmission and the solid angle factor, can be estimated as about 15%. It means that most of the radiation, which did not pass to the laser cell, is converted also to the heat finally. So, we can consider this e-gas value as lower limit for the electron beam energy with accuracy about 20%, which corresponds to the difference between measurements by pressure transducer and calorimeters.

Figure 9a shows typical diode voltage and current waveforms at 95 kV charging voltage. Figure 9b shows calculated waveforms for the diode power and energy. One can see in Figure 9 that there are some oscillations at the beginning of

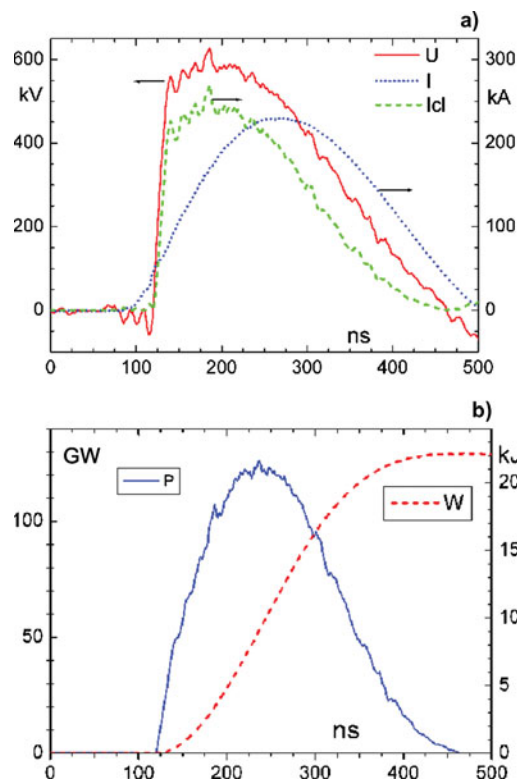


Fig. 9. (Color online) (a) Waveforms of the diode voltage U , diode current I , and one-dimensional space charge limited current I_{cl} at 95 kV charging voltage; (b) calculated traces of the diode power P and energy W .

a voltage pulse. These oscillations arise due to fact that diode voltage is recalculated through measured voltages on stages, measured current (at output of last stage) and inductances between the each stage and the diode. This calculation method provides correct results for settled regime only and not valid for transition regime at the pulse beginning (actually the term “diode voltage” is valid only to the settled regime) but this initial part does not contribute to energetic balance. This initial noise on voltage is due to some jitter in stages firing and voltage reflections.

In Figure 9, one can see that that amplitude of the diode current is close to one-dimensional space charge limited current (SCL current) given by Langmuir-Blodgett law for coaxial diodes (Langmuir & Blodgett, 1923). It means that anode plasma effects are negligible for this diode due to low current density of the electron beam (less than 40 A/cm^2).

Although a numerical solution is easily attainable, at present no analytical form exists for the single-species SCL current in cylindrical diodes in the relativistic regime. Approximate generalization of the Langmuir-Blodgett law for the relativistic regime is given in Zhang *et al.* (2009). Electron beam generation studies were carried out by Roy *et al.* (2009) in high power cylindrical diode in order to investigate the effect of the accelerating gap and diode voltage on the electron beam current. The diode voltage has been varied in Roy *et al.* (2009) from 130 to 356 kV, whereas the current density has been varied from 87 to 391 A/cm^2

Table 1. Generator and electron beam parameters depending on charging voltage

Charging voltage, kV	Peak diode Voltage/current, kV/kA	Diode power/energy GW/kJ	Generator Energy, kJ	Firing delay/Jitter, ns
85	520/195	90/18	27.8	60/6
90	560/215	110/21	31.1	55/4
95	600/230	125/23	34.6	50/4

with 100 ns pulse duration. It was shown in Roy *et al.* (2009) that diode voltage and current do not follow the bipolar space-charge limited flow and beam current is not enhanced by a factor of 1.86 even though there is some formation of anode plasma. It agrees well with our experiments. Cylindrical diode with radially converging electron beam has been also employed in Divall *et al.* (1996) for pumping of Titania KrF laser module.

The charged-particle flow in a self-magnetically insulated cylindrical diode has been studied in Swanekamp *et al.* (2000) through the combination of simulation and analytic techniques. It was shown there that the I - V characteristics of the diode can be divided into three regimes of operation: the SCL regime, a magnetically limited regime where the electron flow is strongly pinched, and a transition regime where the electron flow is weakly pinched. The investigated diode in our experiments can be considered as operating in weakly pinched regime. Deviation of the electron trajectories by self magnetic field does is small.

Electron beam energies, measured by calorimeters and by a pressure jump, were about 8 and 7 kJ, respectively, at 95 kV charging voltage. Homogeneity of the electron beam has been estimated at level of 20% by set of calorimeters and by beam imprint on a radiachromic film placed behind the anode foil. At charging voltage of 95 kV the initial stored energy in the generator is equal to 34.6 kJ. Electron beam energy is about 23 kJ, dissipated energy in the stages cores is about 4 kJ energy losses in the switches and on active resistances of the capacitors is 8.6 kJ. Diode parameters in dependence on charging voltage are summarized in Table 1. One can see from Table 1 that the diode voltage and current depend almost linearly on the charging voltage with deviation less than 4%. It proves stable and reliable operation of all generator elements.

SUMMARY

We have successfully designed and built a multikilojoule electron beam generator on base of new LTD technique that definitely can be considered as the most advanced LTD installation in the world up to now. Intense electron beam generation studies were carried out in a high power cylindrical diode. The measured electron beam current follows

mainly the unipolar SCL flow model. No erosion of the anode material has been observed even after a large number of shots (about 2000 shots at 90–95 kV charging voltage). It is common for us to fire the generator an average of about 10–20 shots per day for several weeks during an experimental run. The generator is reliable, it has been fully incorporated into the hybrid femtosecond XeF (C-A) laser facility, and is routinely used now for the laser research.

REFERENCES

- BASTRIKOV, A.N., VIZIR, V.A., VOLKOV, S.N., DURAKOV, V.G., EFREMOV, A.M., ZORIN, V.B., KIM, A.A., KOVALCHUK, B.M., KUMPYAK, E.V., LOGINOV, S.V., SINEBRYUKHOV, V.A., TSOU, N.V., CHERVYAKOV, V.V., YAKOVLEV, V.P. & MESYATS, G.A. (2003). Primary energy storages based on Linear Transformer Stages. *Laser Part. Beams* **21**, 295–299.
- DIVALL, E.J., EDWARDS, C.B., HIRST, G.J., HOOKER, C.J., KIDD, A.K., LISTER, J.M.D., MATHUMO, R., ROSS, I.N., SHAW, M.J., TONER, W.T., VISSER, A.P. & WYBORN, B.E. (1996). Titania – a 10^{20} W/cm² ultraviolet laser. *J. Mod. Opt.* **43**, 1025–1033.
- ECKSTROM, D.J., NAKANO, H.H., LORENTS, D.C., ROTHMB, T., BETTS, J.A., LAINHART, M.E., DAKIN, D.A. & MAENCHENC, J.E. (1988). Characteristics of electron-beam-excited Xe₂^{*} at low pressures as a vacuum ultraviolet source. *J. Appl. Phys.* **64**, 1679–1690.
- HUMPHRIES, S., Jr. (1986). Principles of Charged Particle Acceleration. New York: Wiley-Interscience, 283–313.
- KARASIK, M., WEAVER, J.L., AGLITSKIY, Y., WATARI, T., ARIKAWA, Y., SAKAIYA, T., OH, J., VELIKOVICH, A.L., ZALESK, S.T., BATES, J.W., OBENSCHAIN, S.P., SCHMITT, A.J., MURAKAMI, M. & AZECHI, H. (2010). Acceleration to high velocities and heating by impact using Nike KrF laser. *Phys. Plasmas* **17**, 056317.
- KIM, A.A., KOVALCHUK, B.M., KUMPYAK, E.V. & TSOU, N.V. (1999). Linear transformer driver with 750-kA current and 400-ns current risetime. *Russian Phys. J.* **42**, 985.
- KIM, A.A., MAZARAKIS, M.G., SINEBRYUKHOV, V.A., KOVALCHUK, B.M., VISIR, V.A., VOLKOV, S.N., BAYOL, F., BASTRIKOV, A.N., DURAKOV, V.G., FROLOV, S.V., ALEXEENKO, V.M., MCDANIEL, D.H., FOWLER, W.E., LECHEN, K., OLSON, C., STYGAR, W.A., STRUVE, K.W., PORTER, J. & GILGENBACH, R.M. (2009). Development and tests of fast 1-MA linear transformer driver stages. *Phys. Rev. ST Accel. Beams* **12**, 050402.
- KOVALCHUK, B.M., ABDULIN, E.N., GRISHIN, D.M., GUBANOV, V.P., ZORIN, V.B., KIM, A.A., KUMPYAK, E.V., MOROZOV, A.V., SKAKUN, V.S., STEPCHENKO, A.S., TARASENKO, V.F., TOLKACHEV, V.S., SHANIN, P.M. & TSOU, N.V. (2003). Linear transformer accelerator for the excimer laser. *Laser Part. Beams*, **21**, 295–299.
- KOVALCHUK, B.M., KHARLOV, A.V., ZHERLITSYN, A.A., KUMPIAK, E.V., TSOY, N.V., VIZIR, V.A. & SMORUDOV, G.V. (2009a). 40 GW linear transformer driver stage for pulse generators of megampere range. *Laser Part. Beams* **27**, 371–378.
- KOVALCHUK, B.M., KHARLOV, A.V., ZORIN, V.B. & ZHERLITSYN, A.A. (2009b). *Rev. Sci. Instrum.* **80**, 083504.
- KRASIK, YA.E., YARMOLICH, D., GLEIZER, J.Z., VEKSELMAN, V., HADAS, Y., GUROVICH, V.Tz. & FELSTEINER, J. (2009). Pulsed plasma electron sources. *Phys. Plasmas* **16**, 057103.
- LANGMUIR, I. & BLODGETT, K. (1923). Currents limited by space charge between coaxial cylinders. *Phys. Rev.* **22**, 347.
- MYERS, M.C., SEETHING, J.D., GIULIANI, J.L., LEHMBERG, R., KEPPEL, P., WOLFORD, M.F., HEGELER, F., FRIEDMAN, M., JONES, T.C., SWANEKAMP, S.B., WEIDENHEIMER, D. & ROSE, D. (2004). Repetitively pulsed, high energy KrF lasers for inertial fusion energy. *Nucl. Fusion*. **44**, S247.
- ROY, A., MENON, R., MITRA, S., SHARMA, V., SINGH, S.K., NAGESH, K.V. & CHAKRAVARTHY, D.P. (2009). Electron beam current in high power cylindrical diode. *Phys. Plasmas*, **17**, 013103.
- SETHIAN, J.D., MEYERS, M., SMITH, I.D., CARBONI, V., KISHI, J., MORTON, D., PEARCE, J., BOWEN, B., SCHLITT, L., BARR, O. & WEBSTER, W. (2000). Pulsed power for a rep-rate, electron beam pumped KrF laser. *IEEE Trans. Plasma Sci.* **28**, 1333.
- SETHIAN, J.D., OBENSCHAIN, S.P., GERBER, K.A., PAWLEY, C.J., SERLIN, V., SULLIVAN, C.A., WEBSTER, W., DENIZ, A.V., LEHECKA, T., MCGEOCH, M.W., ALTES, R.A., CORCORAN, P.A., SMITH, I.D. & BARR, O.C. (1997). Large area electron beam pumped krypton fluoride laser amplifier. *Rev. Sci. Instrum.* **68**, 2357.
- SMITH, I.D. (2004). Induction voltage adders and the induction accelerator family. *Phys. Rev. ST Accel. Beams* **7**, 064801.
- SWANEKAMP, S.B., COMMISSO, R., COOPERSTEIN, J.G., OTTINGER, P.F. & SCHUMERA, J.W. (2000). Particle-in-cell simulations of high-power cylindrical electron beam diodes. *Phys. Plasmas* **7**, 5214.
- TCHEREMISKINE, V.I., SENTIS, M.L. & MIKHEEV, L.D. (2002). Amplification of ultrashort laser pulses in the photolytically driven XeF(C-A) active medium. *Appl. Phys. Lett.* **81**, 403.
- ZHANG, Y., LIU, G., YANG, Z., XING, Q., SHAO, H., XIAO, R., ZHONG, H. & LIN, Y. (2009). Simple solutions for relativistic generalizations of the Child-Langmuir law and the Langmuir-Blodgett law. *Phys. Plasmas* **16**, 044511.
- ZHERLITSYN, A.A., KOVALCHUK, B.M. & SMORUDOV, G.V. (2009). Powerful femtosecond hybrid laser systems with wide aperture amplifiers on base of gas lasers. *Instr. Exper. Techn.* **52**, 802.
- ZVORYKIN, V.D., IONIN, A.A., KONYASHCHENKO, A.V., KOVALCHUK, B.M., KROKHIN, O.N., LOSEV, V.F., MESYATS, G.A., MIKHEEV, L.D., MOLCHANOV, NOVOSELOV, YU.N., SELEZNEV, L.V., SINITSYN, D.V., STARODUB, A.N., TARASENKO, V.F. & YAKOVLENKO, S.I. (2008). Powerful femtosecond hybrid laser systems. *Bull. Tamsk Polytechn. Univ.* **311**, 121.